THE JOURNAL OF BIOLOGICAL CHEMISTRY VOL. 286, NO. 38, pp. 33369–33379, September 23, 2011

Tripartite Motif 24 (Trim24/Tif1α) Tumor Suppressor Protein Is a Novel Negative Regulator of Interferon (IFN)/Signal Transducers and Activators of Transcription (STAT) Signaling Pathway Acting through Retinoic Acid Receptor α (Rarα) Inhibition*[S]

Received for publication, January 27, 2011, and in revised form, July 18, 2011 Published, JBC Papers in Press, July 18, 2011, DOI 10.1074/jbc.M111.225680

Johan Tisserand[1], Konstantin Khetchoumian[2], Christelle Thibault, Doulaye Dembélé, Pierre Chambon[3], and Régine Losson[†]

From the Department of Functional Genomics, Institut de Génétique et de Biologie Moléculaire et Cellulaire (IGBMC), CNRS/INSERM/Université Louis Pasteur, BP 10142, 67404 Illkirch-Cedex, Communauté Urbaine de Strasbourg, France

Recent genetic studies in mice have established that the nuclear receptor coregulator Trim24/Tif1α suppresses hepatocarcinogenesis by inhibiting retinoic acid receptor α (Rara)-dependent transcription and cell proliferation. However, Rara targets regulated by Trim24 remain unknown. We report that the loss of Trim24 resulted in interferon (IFN)/STAT pathway overactivation soon after birth (week 5). Despite a transient attenuation of this pathway by the induction of several IFN/STAT pathway repressors later in the disease, this phenomenon became more pronounced in tumors. Remarkably, *Rara* haplodeficiency, which suppresses tumorigenesis in *Trim24*$^{-/-}$ mice, prevented IFN/STAT overactivation. Moreover, together with Rara, Trim24 bound to the retinoic acid-responsive element of the *Stat1* promoter and repressed its retinoic acid-induced transcription. Altogether, these results identify Trim24 as a novel negative regulator of the IFN/STAT pathway and suggest that this repression through Rara inhibition may prevent liver cancer.

Hepatocellular carcinoma (HCC)[4] is the third leading cause of cancer death worldwide, causing over 660,000 deaths annually (1). Although much is known about the cellular changes that lead to HCC (2) as well as the etiological factors responsible for the majority of the cases (hepatitis B and C viruses infection, aflatoxin exposure, and alcohol abuse, 3), the molecular pathogenesis of HCC remains poorly understood (4, 5).

Initially identified as a fusion partner of B-Raf in T18 oncoprotein in the context of chemically induced HCC in mice (6), tripartite motif (Trim) 24 protein, also known as transcriptional intermediary factor 1α (Tif1α), was subsequently shown to modulate both positively and negatively the transcriptional activities of several nuclear receptors in a ligand-dependent fashion (7–13). Among them, retinoic acid (RA) receptors (Rarα, -β, and -γ) control various biological processes, such as development, proliferation, and differentiation. Upon ligand binding (RA, the active derivative of vitamin A), Rars activate transcription of their target genes, including *Cyp26a1* encoding an RA catabolic enzyme (for a review, see Ref. 14). Because many transcription factors and signaling molecules are targeted by Rars, the RA pathway can interfere with several other pathways. In particular, RA was demonstrated to synergize with interferon (IFN)/signal transducers and activators of transcription (STAT) signaling and thus to potentate inflammation (Ref. 15 and references therein).

The physiological significance of Trim24-mediated nuclear receptor repression has been demonstrated by recent genetic studies in mice revealing that Trim24 is a potent liver-specific tumor suppressor (16–18). Specifically, it was shown that *Trim24*$^{-/-}$ mutant mice are highly predisposed to the development of both spontaneous and chemically induced HCC. Hepatocyte-specific, inducible inactivation of Trim24 revealed that it acts as a cell-autonomous tumor suppressor, maintaining the quiescent state of hepatocytes (18). Similarly to models of liver cancer development in humans, the development of HCC in *Trim24*$^{-/-}$ mice is a multistage process, validating the utility of this mouse model for understanding basic mechanisms of hepatocarcinogenesis in humans (2, 16, 18, 19). As soon as 3

* This work was supported in part by the CNRS, INSERM, Agence Nationale de la Recherche Grant ANR06-BLAN-0377, Association pour la Recherche contre le Cancer (ARC), Ligue Nationale Contre le Cancer, and the Institut National du Cancer (INCa; Project ARTOn).

This manuscript is dedicated to Régine Losson who died untimely a year ago. She was a wonderful colleague and an outstanding scientist. Together with her student Bertrand Le Douarin, who tragically disappeared 10 years ago, they discovered the TIF family in 1994.

† Deceased.

[S] The on-line version of this article (available at http://www.jbc.org) contains supplemental Figs. S1–S3 and Tables S1–S4.

[1] Supported by fellowships from the Ministère de la Recherche et des Technologies, ARC, INCa, and ARI (Agence Régionale de l'Innovation). Present address: Inst. de Recerca Biomèdica Barcelona (IRBB), Parc Científic de Barcelona, c/ Baldiri Reixac 10, 08028 Barcelona, Spain.

[2] Present address: Laboratoire de Génétique Moléculaire, Inst. de recherches cliniques de Montréal (IRCM), Montréal, H2W 1R7 Quebec, Canada.

[3] To whom correspondence should be addressed. Tel.: 33-3-88-65-32-13; E-mail: chambon@igbmc.fr.

[4] The abbreviations used are: HCC, hepatocellular carcinoma; KO, knock-out (*Trim24*$^{-/-}$); R, rescued (*Trim24*$^{-/-}$*Rara*$^{+/-}$); RA, retinoic acid; Rar, retinoic acid receptor; F-, FLAG-tagged; Rara, retinoic acid receptor α; Trim, tripartite motif; Tif1α, transcriptional intermediary factor 1α; Hprt, hypoxanthine-guanine phosphoribosyltransferase; RARE, RA-responsive element; ISG, IFN-stimulated gene; qPCR, quantitative RT-PCR; Rxra, retinoid X receptor α.

weeks after birth, while hepatocytes are terminating their postnatal development and are entering into quiescence, the first manifestations of the disease, namely increased hepatocyte proliferation, could be observed in Trim24-deficient mice. Increased hepatocyte ploidy (week 14) and preneoplastic (clear cell foci of cellular alterations) and neoplastic lesions (hepatocellular adenomas and carcinomas) then appear with a highly reproducible kinetics (16–18). Remarkably, the whole process of HCC development in Trim24-deficient mice was shown to depend on overactivated RA signaling. Indeed, all pathological manifestations of Trim24-deficient liver disease described above are completely suppressed upon simultaneous loss of a single copy of the *Rara* gene ($Trim24^{-/-}Rara^{+/-}$ mutant mice; Refs. 16 and 17). Consistent with this, administration of pharmacological doses of RA stimulates hepatocyte proliferation in wild-type mice, whereas injection of Rar antagonists restore normal hepatocyte proliferation rate in $Trim24^{-/-}$ mice (16, 17). These findings provided the first evidence that Rara can function as an oncogene *in vivo* and prompted us to examine the molecular mechanisms by which Rara overactivation stimulates hepatocyte proliferation. We have now characterized Trim24/Rara common downstream targets in hepatocytes and discovered that Trim24 is a novel negative regulator of the IFN/STAT signaling pathway, acting through Rara inhibition. Moreover, we found that the overactivation of IFN/STAT signaling pathway in $Trim24^{-/-}$ livers tightly correlates with RA-mediated hepatocarcinogenesis.

EXPERIMENTAL PROCEDURES

Mice and Tissue Samples—Generation of $Trim24^{-/-}$ and $Trim24^{-/-}Rara^{+/-}$ mice has been described previously (16). Colonies of both lines were maintained under specific pathogen-free conditions at the Mouse Clinical Institute of the Institut de Génétique et de Biologie Moléculaire et Cellulaire. Harvesting of mouse liver tissues was done as described by Khetchoumian *et al.* (16). Livers were rapidly excised and washed in PBS, and tissue portions were frozen in liquid nitrogen and stored at −80 °C until use for RNA extraction and Western blot analysis. A liver sample (left median lobe or a sample with a macroscopically visible tumor) was fixed in 4% paraformaldehyde and paraffin-embedded, and another sample was optimal cutting temperature-included and frozen for routine histology. All liver samples were subjected to histopathological evaluation before analysis. All animal procedures were approved by the French Ministry of Agriculture (Agreement B67-218-5) according to guidelines in compliance with the European legislation on care and use of laboratory animals.

RNA Isolation and Quantitative RT-PCR—Total RNA was isolated from liver tissues and cell lines using an RNeasy kit (Qiagen) and TRIzol reagent (Invitrogen), respectively. Five micrograms of RNA were used for cDNA synthesis using oligo$(dT)_{24}$ primer and Superscript II reverse transcriptase (Invitrogen) according to the manufacturer's instructions. The final product was then diluted 80 times, and 4 μl were mixed with forward and reverse primers listed in supplemental Table S4 (each primer at 250 nM final concentration) and 5 μl of SYBR Green Master Mix (Qiagen). Real time PCR was performed using the LightCycler 1.5 system (Roche Applied Science). Each reaction was performed in triplicate, and the relative expression level of each gene was normalized to the hypoxanthine-guanine phosphoribosyltransferase (*Hprt*) level.

Microarray Experiments—Gene expression profiling was performed using the Affymetrix GeneChip® Mouse Genome 430 2.0 microarrays. Total RNA was isolated using an RNeasy kit (Qiagen) and quality-controlled by capillary electrophoresis (Agilent 2100 Bioanalyzer and RNA 6000 LabChip® kit). cDNA and cRNA synthesis and labeling as well as array hybridization were performed at the Affymetrix facility of the Institut de Génétique et de Biologie Moléculaire et Cellulaire according to the manufacturer's instructions (Affymetrix). Raw microarray data were analyzed using the GeneChip Operating Software (GCOS) for normalization, detection calls, and expression values. A present, absent, or marginal call and a value of signal intensity were given for each gene. Changes in expression were first analyzed by analysis of variance and Newman-Keuls (for samples from 5-week-old livers) or Student's *t* test (for samples from 14-week-old livers and tumors). Each gene was identified as up-regulated, down-regulated, or not changed based on significance ($p < 0.01$). We controlled the false discovery rate using sample permutations (false discovery rate <0.014). To eliminate unexpressed genes, a gene must have had a presence call in at least three of the four mutant (or wild-type (WT)) samples. Finally, the average signal intensity of replicates was used to calculate -fold change. We selected the most significant changes with an arbitrary threshold of 1.7. In brief, the differentially expressed genes were selected based on $p < 0.01$, presence call >0.75, and -fold change >1.7. This set of genes was further filtered to eliminate genes without an Entrez Gene ID and to obtain a single entry for genes represented by multiple probe sets. Average linkage hierarchical clustering was performed using Cluster software. Biological process assignments were made using the DAVID bioinformatics tool and Ingenuity Pathway Analysis software.

Liver Protein Extraction and Western Blot Analysis—Liver whole-cell extracts were prepared as described previously (20). Protein concentration was determined using Bio-Rad protein assay reagent. Equal amounts of proteins (100–200 μg) were separated by SDS-PAGE and processed for Western blotting as described by Khetchoumian *et al.* (20). Rabbit polyclonal antibodies recognizing Stat1 (E-23) and Irf1 (C-20) from Santa Cruz Biotechnology (Santa Cruz, CA) and a monoclonal antibody against β-tubulin (1TUB1A2; a gift from Dr. M. Oulad-Abdelghani, Institut de Génétique et de Biologie Moléculaire et Cellulaire) were used as primary antibodies. Peroxidase-conjugated goat anti-rabbit IgG or goat anti-mouse IgG (Jackson ImmunoResearch Laboratories) were used as secondary antibodies. Detection was carried out using an enhanced chemiluminescence (ECL) kit (Amersham Biosciences).

Cell Culture and Transfection—The murine non-transformed hepatocyte cell line AML12 was described previously (21) and obtained from the European Collection of Cell Cultures. Cells were grown at 37 °C in a humidified incubator containing 5% CO_2, 95% air in Dulbecco's minimal essential medium (DMEM)/F-12 medium (1:1) supplemented with 10% fetal bovine serum, 100 nM dexamethasone, 50 μg/ml gentamicin sulfate, and a mixture of insulin, transferrin, and selenium

(5 μg/ml). Quantitative RT-PCR and chromatin immunoprecipitation (ChIP) experiments were carried out using cells treated with vehicle (ethanol) or 1 μm all-*trans*-retinoic acid (Sigma) in medium containing delipidated serum.

AML12 cells (2×10^6) were transfected using the Amaxa Nucleofactor reagent (Amaxa Biosystems, Lonza) with pSG5-based expression vectors for Rara (0.125 μg) and Rxra (0.125 μg) together with a control empty vector, FLAG-tagged Trim24 wild type (F-Trim24), or Trim24L730A/L731A (8) (4.75 μg) according to the manufacturer's instructions.

ChIP Assays—ChIP assays were performed as described previously (16) except for some modifications. In brief, cells (2×10^7) were cross-linked with 1% formaldehyde (v/v) for 10 min at 37 °C, resuspended in 450 μl of SDS lysis buffer (Upstate), and incubated at 37 °C for 10 min. Cell lysates were sonicated to obtain DNA fragments of 200–500 bp using the Bioruptor from Diagenode. Sonicated samples were then cleared by centrifugation at 13,000 rpm for 15 min at 4 °C, and 20% of the cleared supernatant was kept for subsequent purification of input genomic DNA. The remaining chromatin (350 μl) was first precleared overnight with 50 μl of Protein G-Sepharose beads at 4 °C. The beads were removed by centrifugation at 2,000 rpm for 2 min, and 50 μg of sonicated chromatin were then incubated with 25 μl of M2 FLAG affinity agarose beads (Sigma) or non-conjugated beads as a negative control. ChIP was performed by incubation at 4 °C for 2 h in 1 ml of ChIP dilution buffer (16.7 mM Tris-HCl, pH 8.0, 167 mM NaCl, 1.2 mM EDTA, 1.1% Triton X-100, 0.01% SDS). The immunoprecipitates were collected by centrifugation and sequentially washed in 3 × 1 ml of ChIP low salt buffer (20 mM Tris-HCl, pH 8.0, 150 mM NaCl, 2 mM EDTA, 1% Triton X-100, 0.1% SDS), 3 × 1 ml of ChIP high salt buffer (20 mM Tris-HCl, pH 8.0, 500 mM NaCl, 2 mM EDTA, 1% Triton X-100, 0.1% SDS), 3 × 1 ml of LiCl buffer (10 mM Tris-HCl, pH 8.0, 250 mM LiCl, 1 mM EDTA, 1% Nonidet P-40, 1% sodium deoxycholate), and in 2 × 1 ml of TE buffer (10 mM Tris-HCl, pH 8.0, 1 mM EDTA) before being eluted in two consecutive steps by adding 250 μl of elution buffer (1% SDS, 100 mM $NaHCO_3$) at each step. Eluates and input chromatin were incubated at 65 °C for a minimum of 4 h in the presence of 0.2 M NaCl to reverse cross-linking of the chromatin. Proteins were digested by addition of 10 μl of 1 M Tris-HCl, pH 6.8; 10 μl of 0.5 M EDTA; and 20 μg of proteinase K and incubation at 42 °C for 1 h. The DNA was recovered by phenol/chloroform extraction and coprecipitation with GlycoBlue (Ambion), dissolved in 100 μl of TE buffer, and analyzed by quantitative PCR with primers flanking the RA-responsive element (RARE) regions of the *Stat1* and *Cyp26a1* promoters (22, 23) and the *Hprt* promoter as a control (see supplemental Table S4). Trim24 occupancy of the RARE-containing regions of *Stat1* and *Cyp26a1* promoters was quantified by normalizing the PCR signals from the immunoprecipitation samples to the PCR signals obtained from both the input DNA and the promoter region of the *Hprt* housekeeping gene, which showed no change in expression in $Trim24^{-/-}$ livers or F-Trim24-transfected AML12 cells[5] and therefore was used as a negative control. Normalization in this way is an effective method to significantly reduce interassay variation arising from extensive manipulations of the chromatin during the experimental processes. Statistical significance was determined by using the Student's *t* test on three independent experiments, each performed in triplicate.

Immunohistofluorescence and Image Analysis—The number of macrophages/Kupffer cells present in the liver was determined using rat anti-mouse CD68 (macrosialin) antibody (Serotec, Raleigh, NC) and fluorescence microscopy. Briefly, frozen tissue sections were dried for 15 min, hydrated at room temperature in PBS, and then fixed in cold acetone for 10 min at 4 °C. After three sequential 5-min washes in PBS, 1% Triton X-100 (PBT), sections were blocked in 1% BSA. Primary antibody targeting CD68 (1:50) was then applied to the sections for 16 h at 4 °C in a humidified chamber. After washing in PBT and PBS, the slides were incubated with Cy3-coupled anti-rat secondary antibody (Jackson ImmunoResearch Laboratories 112-165-143; 1:500) for 30 min at room temperature and washed three times in PBT and for 2 min in PBS. Sections were mounted with Mowiol containing DAPI (10 mg/ml). Image acquisitions were performed using a fluorescence microscope (Leica DMLB 30T, Leica Microsystems, Wetzlar Germany), and the number of CD68-positive cells per centrilobular field was determined using CoolSNAP software. Five centrilobular areas were counted per tissue sample.

RESULTS

In an effort to identify Trim24 and Rara downstream targets that may play a role in liver carcinogenesis, we analyzed transcriptomic changes that take place in early precancerous livers of $Trim24^{-/-}$ mutants that occurred in a Rara gene dosage-dependent manner. Gene expression profiling experiments were performed comparing liver transcriptomes of week 5 $Trim24^{-/-}$ knock-out (KO) or $Trim24^{-/-}Rara^{+/-}$ "rescued" (R) mice with transcriptomes of WT littermates using the Affymetrix Mouse Genome 430 2.0 microarrays (GSE19675). At this age, no overt liver pathology was detectable in *Trim24* KO mice (supplemental Fig. S1), but these mice were characterized by an increased hepatocyte proliferation and an overexpression of numerous RA-responsive genes (16, 17). Because no such defects were observed in age-matched $Trim24^{-/-}Rara^{+/-}$ rescued mice that are not prone to tumor development (17), we expected to identify oncogenic downstream Rara targets among genes deregulated in KO but not R livers. To identify differentially expressed transcripts, gene lists from different samples were filtered according to multiple criteria as described under "Experimental Procedures." Briefly, transcripts detectable in at least three of the four samples showing a -fold change ≥1.7 with a *p* value ≤0.01 were extracted, giving rise to 194 and 80 unique genes differentially expressed between KO/WT and R/WT, respectively (Fig. 1, *A* and *B*). Hierarchical clustering allowed distinguishing six clusters from these gene lists (Fig. 1*A*). Cluster 5 was by far the largest, containing 122 overexpressed genes in *Trim24* KO livers only, including HCC markers Afp and H19 (3.2- and 1.75-fold, respectively; supplemental Table S1). 145 of the 194 genes deregulated in *Trim24* KO livers exhibited no significant

[5] J. Tisserand, K. Khetchoumian, P. Chambon, and R. Losson, unpublished data.

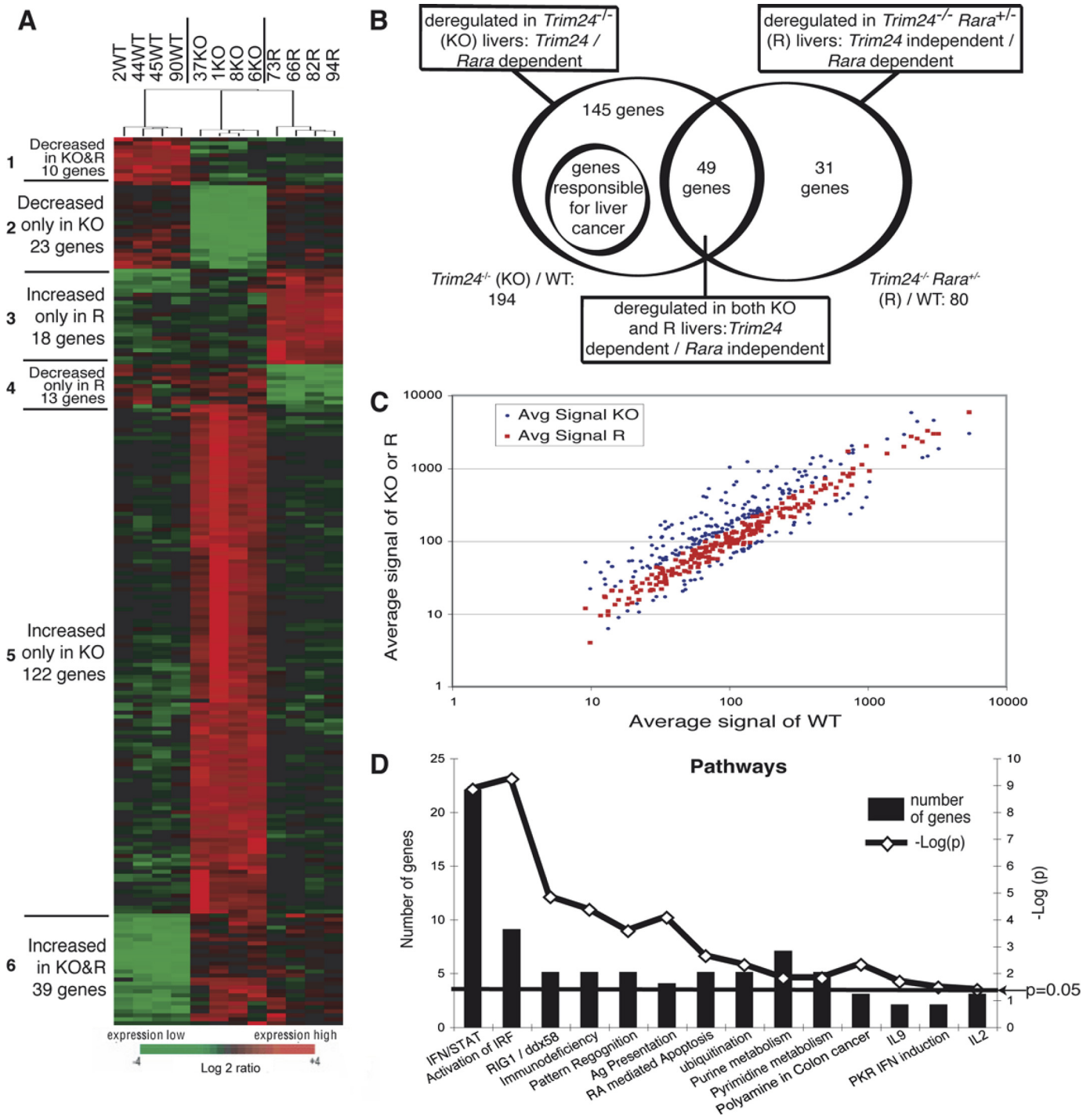

FIGURE 1. **Transcriptomics analysis at week 5.** *A*, average linkage hierarchical clustering representing the expression profiles of genes deregulated in week 5 *Trim24*$^{-/-}$ (KO) and *Trim24*$^{-/-}$*Rara*$^{+/-}$ (R) livers. Each *column* represents a liver sample, and each *row* represents a gene. *Red* and *green* represent up- and down-regulation, respectively. Six major clusters (*1–6*) are highlighted at *left* (see supplemental Table S1 for the complete list). *B*, Venn diagram indicating the relationships between gene alterations in week 5 KO and R livers with respect to Trim24 and Rara dependence. *C*, scatter graph showing the extent of the rescue: average (*Avg*) expression of *Trim24*/*Rara*-dependent genes in mutants (*blue*, KO; *red*, R) is a function of their expression level in WT. *D*, Ingenuity Pathway Analysis identification of *Trim24*/*Rara*-dependent genes. The *bars* and the *curve* represent the number of genes and −log(*p* value), respectively. Pathways with −log(*p*) over the base line are significantly altered ($p < 0.05$). *Ag*, antigen; *IRF*, INF Regulated Factor; *PKR*, Protein kinase R; *RiG1*, Retinoic Acid inducibile Gene 1; *ddx58*, Asp-Glu-Ala-Asp (DEAD) box protein 58; *IL*, Interleukin.

change in *Trim24*$^{-/-}$*Rara*$^{+/-}$ livers, indicating that their deregulation in the absence of *Trim24* is reversed upon deletion of a single copy of Rara (Fig. 1, *B* and *C*). These genes were therefore referred to as Trim24/Rara-dependent. Of the 80 deregulated genes in R livers, 31 genes did not show any significant deregulation in *Trim24* KO livers and were referred to as Trim24-independent/Rara-dependent, whereas the remaining 49 genes were deregulated in both *Trim24* KO and *Trim24*$^{-/-}$ *Rara*$^{+/-}$ R livers and were referred to as Trim24-dependent/Rara-independent. The complete gene lists are presented in

supplemental Table S1. Taken together, these results identify Rara as a major target of Trim24 repression in the liver.

IFN/STAT Activation at Week 5—The DAVID bioinformatics tool was used to identify biological processes that could be controlled by Trim24/Rara-dependent genes and revealed a significant enrichment in genes involved in immune-related processes (supplemental Table S2). Using the Ingenuity Pathway Analysis software, we subsequently identified the IFN/STAT signaling pathway ($p < 1.5 \times 10^{-9}$) as well as several IFN/STAT-associated pathways (IFN Regulatory Factor, RIG1, immunodeficiency, antigen presentation, Protein Kinase R IFN induction) as being the most significantly altered (Fig. 1*D*). This signaling pathway plays key roles in mediating the antiviral, antigrowth, and immunomodulatory activities of IFNs (for a review, see Ref. 24). The transduction of IFN signals in target cells involves activation of Type I and Type II IFN receptors and receptor-associated Janus-activated kinase (JAK), which in turn leads to activation and nuclear translocation of STAT proteins and results in the transcription of IFN-stimulated genes (ISGs). Comparison of our list of Trim24/Rara-dependent genes with the ISG Database (25) showed 67 overlapping genes with 66 being up-regulated in *Trim24* KO livers (1.7–10.5-fold; Table 1). Among them, we identified several components of the IFN signaling pathway (*e.g. Stat1* (3.0-fold), *Irf7* (4.7-fold), and *Irf9* (1.8-fold)) and numerous ISGs, such as *Ifit1* (10.5-fold), *Ifit3* (9.3-fold), *Oas1* (5.0-fold), and *Isg15* (7.5-fold). Activation of the IFN/STAT pathway was confirmed by quantitative RT-PCR (qPCR) in all *Trim24* KO liver samples. qPCR analysis also revealed up-regulation of *Irf1*, an important regulator of the IFN pathway (26), and confirmed that expression of *Irf1*, *Stat1*, *Oas1*, and *Ifit1* is not altered in the livers of age-matched $Trim24^{-/-}Rara^{+/-}$ mutants, indicating that their deregulation in the absence of Trim24 is correlated with Rara activity (Fig. 2*A*). Importantly, overexpressions of Stat1 (2.2-fold) and Irf1 (2.3-fold) in *Trim24* KO livers were also confirmed at the protein level (Fig. 2*B*). Knowing that phosphorylation of Stat1 at Ser-727 is a key event of IFN/STAT activation, we investigated this phosphorylation level by Western blotting. We showed an accumulation of phosphorylated Stat1 (Ser-727) in $Trim24^{-/-}$ but not in $Trim24^{-/-}Rara^{+/-}$ livers at week 5 (2.1-fold; Fig. 2*B*). Taken together, all these data provide compelling evidence for a Rara-dependent overactivation of the IFN/STAT pathway in early precancerous livers of *Trim24* KO mice.

Adaptive Responses at Week 14—We next investigated whether the activation of the IFN/STAT pathway in *Trim24* KO livers is maintained at a later stage of the disease. At week 14, *Trim24* KO mice were characterized by increased hepatocyte proliferation and ploidy (16–18). Liver transcriptomes of week 14 *Trim24* KO and control WT littermates ($n = 5$) were determined using the Affymetrix Mouse Genome 430 2.0 microarrays (GSE19675). Only 90 genes were found to be deregulated in the *Trim24* KO liver samples (-fold change ≥1.7, $p \leq 0.01$): 65 genes were up-regulated and 25 were down-regulated (Fig. 3*A*). Surprisingly, although HCC markers Afp and H19 remained overexpressed, several up-regulated genes correspond to well documented growth inhibitors, such as *Cdkn1a* (p21; 7.0-fold; Ref. 27), *Bmyc* (2.7-fold; Ref. 28), and *Hnf6*/*One-cut1* (4.5-fold; Refs. 29 and 30). Overexpression of these growth inhibitors in hyperproliferating week 14 Trim24-deficient hepatocytes suggests the existence of an adaptive mechanism activated by the liver to fight against hyperproliferation. However, ectopic expression of growth inhibitors is known to alter hepatocyte homeostasis and in particular to lead to increased ploidy (31, 32).

Overall, qPCR analyses revealed that only 14.6% of genes deregulated in week 14 KO livers were Rara-dependent (74.7% at week 5; supplemental Fig. S2A). Moreover, whereas 32.6% of week 5 Trim24-dependent/Rara-independent genes remained deregulated at week 14, only 3.4% of Trim24/Rara-dependent genes were still deregulated at this later stage (supplemental Fig. S2B). Considering that KO but not R livers are prone to tumor development, these results suggest that adaptive mechanisms occur to specifically fight against deleterious Trim24/Rara-dependent deregulations. Supporting this idea, RA pathway hyperactivation that has been described to promote hepatocarcinogenesis was markedly attenuated at week 14 as revealed by the overlapping of our list of deregulated genes with the Balmer and Blomhoff (33) RA target gene database (supplemental Fig. S2C). Likewise, of the 90 aberrantly expressed genes in week 14 KO livers, only 10 genes were present in the ISG Database (Ref. 25 and Fig. 3*B*), including *Usp18*/*Ubp43* recently described as a negative regulator of IFN signaling (34). We carried out qPCR validation for *Usp18* (Fig. 3*C*) and investigated the expression levels of four additional negative regulators of the IFN/STAT pathway: *Socs1*, *Socs2* (35), *Pias1*, (36), and *Pp2ac* (37). Contrary to the situation at week 5, *Socs1* and *Socs2* both exhibited increased expression in KO livers (2.0- and 1.8-fold) and may thus be responsible for the marked attenuation of the IFN/STAT pathway observed at week 14 as compared with week 5 *Trim24* KO livers (Table 1). Taken together, these results show that the RA and IFN/STAT pathways are synchronized and strongly suggest the activation of adaptive response in reaction to Trim24/Rara-dependent tumorigenic deregulations at week 14. If confirmed and generalized, this feed back mechanism (occurring while HCC marker overexpressions still allow diagnosis of HCC predispositions) could be targeted (and promoted) in future cancer-preventive therapies.

IFN/STAT Activation in HCC—This attenuation led us to examine the status of the IFN/STAT pathway in HCCs from *Trim24* KO mice (GSE9012; Ref. 17). 129 components of the IFN/STAT pathway, including the IFNγ receptors 1 (*Ifngr1*; 3.2-fold) and 2 (*Ifngr2*; 6.1-fold), *Jak2* (2.3-fold), *Stat1* (4.7-fold), and *Stat2* (2.1-fold) as well as numerous ISGs common to week 5 Trim24/Rara-dependent genes were found to be deregulated in HCCs (Table 1 and supplemental Table S3). We validated a subset of these genes by qPCR and identified a decrease in expression of the negative regulators *Socs1* and *Socs2* (2.1- and 1.7-fold; supplemental Fig. S3). Therefore, the progression of Trim24-deficient hepatocytes toward HCC seems to require reactivation of the IFN/STAT pathway (Fig. 3*D*). In agreement with this idea, a transcriptomics analysis of 43 human HCCs revealed that 65% of tumors (28 HCCs) exhibit overexpression of ISGs (38). Interestingly, we noticed that Trim24 down-regu-

TABLE 1

Interferon signaling genes deregulated in livers of *Trim24*$^{-/-}$ mice in a *Rara* gene dosage-dependent manner and analysis of their expression at week 14 and in *Trim24*$^{-/-}$ HCC

Genes up- or down-regulated by a factor >1.7 with a p value <0.01 in livers of five *Trim24*$^{-/-}$ but not *Trim24*$^{-/-}$*Rara*$^{+/-}$ mice identified on Affymetrix 430 2.0 microarrays (see supplemental Table S1) and selected from the interferon-regulated gene database are shown.

Gene symbol	Description	Affy ID	-Fold change[a]		
			Week 5	Week 14	Tumors
2810417H13Ri	RIKEN cDNA 2810417H13 gene	1419153_at	1.87	—	—
A630077B13Ri	RIKEN cDNA A630077B13 gene	1436576_at	2.81	—	—
Agrn	Agrin	1426670_at	1.87	—	—
Apol9b	Apolipoprotein L 9b	1424518_at	3.27	—	—
BC013672	cDNA sequence BC013672	1451777_at	4.29	—	—
Blnk	B-cell linker	1451780_at	4.14	—	4.92
Bst2	Bone marrow stromal cell antigen 2	1424921_at	2.35	—	—
Cfhr1	Complement factor H-related 1	1419436_at	2.08	—	—
Csrp1	Cysteine- and glycine-rich protein 1	1425811_a_at	1.81	—	—
Cxcl10	Chemokine (CXC motif) ligand 10	1418930_at	4.37	—	—
Ddx58	DEAD (Asp-Glu-Ala-Asp) box polypeptide 58	1436562_at	1.91	—	—
Dhx58	DEXH (Asp-Glu-*X*-His) box polypeptide 58	1451426_at	4.33	—	—
Epsti1	Epithelial stromal interaction 1	1454169_a_at	3.19	—	—
Fbn1	Fibrillin 1	1460208_at	2.70	—	—
Gbp1	Guanylate nucleotide-binding protein 1	1420549_at	2.79	—	—
Gbp2	Guanylate nucleotide-binding protein 2	1435906_x_at	4.00	—	—
Gbp3	Guanylate nucleotide-binding protein 3	1418392_a_at	5.16	—	—
Glul	Glutamate-ammonia ligase (glutamine synthetase)	1426235_a_at	0.58	0.52	0.12
Herc5	Hect domain and RLD 5	1438037_at	5.99	—	—
Ifi27	Interferon α-inducible protein 27	1426278_at	3.58	—	—
Ifi35	Interferon-induced protein 35	1445897_s_at	2.14	—	—
Ifi44	Interferon-induced protein 44	1423555_a_at	6.47	—	5.64
Ifi47	Interferon γ-inducible protein 47	1417292_at	3.13	—	—
Ifih1	Interferon induced with helicase C domain 1	1426276_at	2.29	—	1.99
Ifit1L	Interferon-induced protein with tetratricopeptide repeats	1450783_at	10.50	—	6.13
Ifit2	Interferon-induced protein with tetratricopeptide repeats	1418293_at	5.28	—	—
Ifit3	Interferon-induced protein with tetratricopeptide repeats	1449025_at	9.31	—	—
Igtp	Interferon γ-induced GTPase	1417141_at	2.73	—	—
Iigp1	Interferon-inducible GTPase 1	1419042_at	1.87	—	2.37
Iigp2	Interferon-inducible GTPase 2	1417793_at	2.82	—	—
Irf7	Interferon regulatory factor 7	1417244_a_at	4.67	—	1.71
Irf9	Interferon regulatory factor 9	1421322_a_at	1.79	—	1.72
Irgm	Immunity-related GTPase family, M	1418825_at	2.37	—	—
Isg15	ISG15 ubiquitin-like modifier	1431591_s_at	7.54	—	—
Lgals3	Lectin, galactose-binding, soluble 3	1426808_at	2.79	—	—
Lgals3bp	Lectin, galactoside-binding, soluble, 3-binding protein	1448380_at	2.20	—	2.73
Ly6a	Lymphocyte antigen 6 complex, locus A	1417185_at	5.24	—	—
Mov10	Moloney leukemia virus 10	1416380_at	1.73	—	2.12
Ms4a4c	Membrane-spanning 4 domains, subfamily A, member 4	1450291_s_at	5.70	—	—
Myh10	Myosin, heavy polypeptide 10, non-muscle	1452740_at	1.94	—	—
Nmi	N-myc (and STAT) interactor	1425719_a_at	1.88	—	—
Numa1	Nuclear mitotic apparatus protein 1	1438027_at	3.59	—	—
Oas1a	2,5-Oligoadenylate synthetase 1A	1424775_at	5.05	1.84	6.02
Oasl1	2,5-Oligoadenylate synthetase-like 1	1424339_at	5.53	—	1.94
Parp12	Poly(ADP-ribose) polymerase family, member 12	1426774_at	2.33	—	—
Phf11	PHD finger protein 11	1438868_at	1.86	—	—
Plac8	Placenta-specific 8	1451335_at	1.87	—	—
Plec1	Plectin 1	1452178_at	1.75	—	—
Prps2	Phosphoribosyl pyrophosphate synthetase 2	1420638_at	1.79	—	—
Psmb10	Proteasome (prosome, macropain) subunit, β type 10	1448632_at	1.81	—	—
Psmb8	Proteasome (prosome, macropain) subunit, β type 8	1422962_a_at	2.08	—	—
Psmb9	Proteasome (prosome, macropain) subunit, β type 9	1450696_at	2.84	—	—
Rtp4	Receptor transporter protein 4	1418580_at	3.57	—	—
S100a11	S100 calcium-binding protein A11 (calgizzarin)	1460351_at	2.51	3.66	17.15
Samd9l	Sterile α motif domain-containing 9-like	1460603_at	2.66	—	—
Samhd1	SAM domain and HD domain, 1	1418131_at	1.74	—	—
Scotin	Scotin gene	1423986_a_at	2.44	—	—
Stat1	Signal transducer and activator of transcription 1	1450033_a_at	3.00	—	4.72
Tap1	Transporter 1, ATP-binding cassette, subfamily B (MDR)	1416016_at	2.90	—	—
Tgfbi	Transforming growth factor, β induced	1448123_s_at	1.71	—	—
Tgtp	T-cell-specific GTPase	1449009_at	5.74	—	—
Tlr2	Toll-like receptor 2	1419132_at	1.92	—	—
Trafd1	TRAF type zinc finger domain-containing 1	1428346_at	1.90	—	—
Trim26	Tripartite motif protein 26	1424929_a_at	1.72	—	—
Trim34	Tripartite motif protein 34	1421550_a_at	3.95	—	2.88
Tyki	Thymidylate kinase family LPS-inducible member	1450484_a_at	4.44	—	—
Ube1l	Ubiquitin-activating enzyme E1-like	1426970_a_at	2.61	—	—
Usp18	Ubiquitin-specific peptidase 18	1418191_at	4.88	2.40	5.72

[a] -Fold change values correspond to the average of the values for all the mutant (or tumor)/control sample comparisons (n = 4 or 5); —, does not meet the criteria of statistical significance. HD, Hydrolase Domain; MDR, MultiDrug Resistance; PHD, Plant HomeoDomain; SAM, Sterile Alpha Mol; TRAF, Tumor Necrosis Factor (TNF) Receptor Associated Factor; ISG, INF Stimulated Gene; RLD, Regulator of Chromosome condensation 1 (RCC1)-like Domain.

lation is part of a highly discriminative transcriptional signature of this tumor subgroup (Fig. 3*D*). Collectively, these data strongly implicate overexpression of the IFN/STAT pathway as an important evolutionarily conserved component of hepatocarcinogenesis (Fig. 3*D*).

Trim24 Represses IFN/STAT Pathway Induction by RA—IFNs and RA are able to potentiate each other to induce biological responses (15 and references therein). This RA/IFN synergy is mediated at least in part by an increase of the Stat1 level upon RA treatment (39). Supporting the idea that Rars could directly

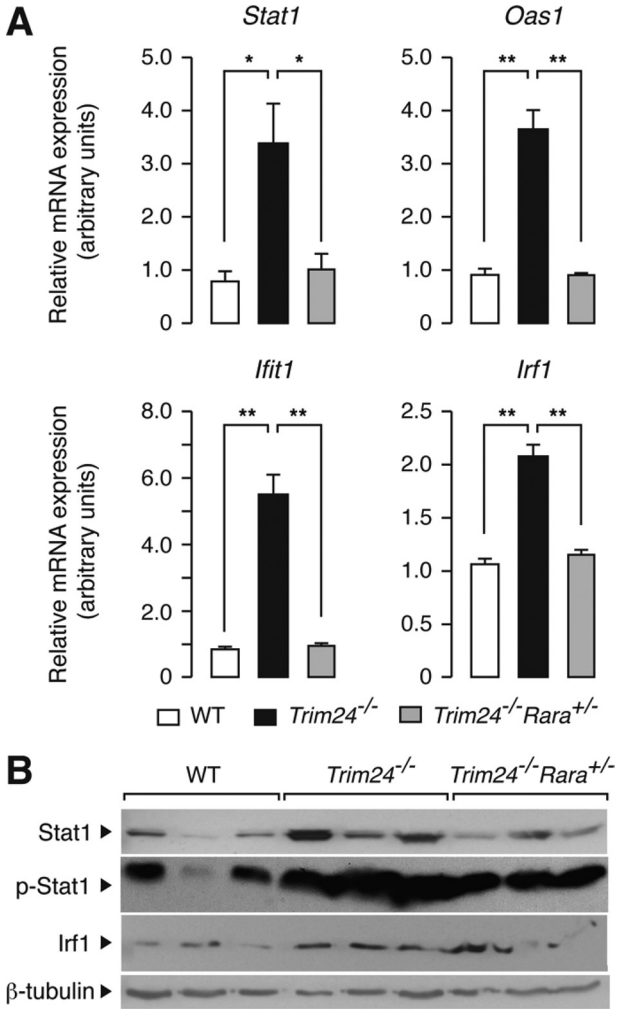

FIGURE 2. **Validation of deregulated expression of genes involved in IFN/STAT signaling pathway.** *A*, qPCR experiments confirming that *Stat1*, *Oas1*, *Ifit1*, and *Irf1* are up-regulated in livers of week 5 $Trim24^{-/-}$ but not $Trim24^{-/-}Rara^{+/-}$ mice. Expression was analyzed in triplicate and is relative to *Hprt* (*Error bars* represent standard error; *, $p < 0.01$; **, $p < 0.001$). *B*, immunoblot analysis of liver protein extracts from week 5 $Trim24^{-/-}$, $Trim24^{-/-}Rara^{+/-}$, and control (WT) mice using the indicated antibodies against Stat1, phosphorylated Stat1 (*p-Stat1*) (Ser-727), and Irf1; β-tubulin was used as a loading control (see "Experimental Procedures"). Western blots were performed in triplicate with liver samples from three different animals.

regulate *Stat1* transcription, an RARE was identified in the promoter region of *Stat1* (22). This led us to examine the effect of RA on *Stat1* expression in the murine non-transformed hepatocyte cell line AML12, which was transiently transfected with an expression vector for Rara and its heterodimeric partner Rxra. Similarly to the well known direct RA target genes *Cyp26a1* and *Stra6*, *Stat1* was rapidly up-regulated after 3 h of treatment with RA, whereas longer treatment was required for the induction of *Stat1* downstream targets *Irf1*, *Oas1*, and *Ifit1* (Fig. 4*A*). Coexpression of Trim24 led to a significant attenuation of the RA-induced increase of mRNA levels of all genes tested (Fig. 4*A*). Importantly, a Trim24 mutant that does not interact with Rara (Trim24L730A/L731A; Ref. 8) lost its ability to repress RA-mediated transactivation (Fig. 4*A*). These results convincingly show that Trim24 can inhibit the RA-dependent activation of the IFN/STAT pathway in hepatic cells and demonstrate that this down-regulation requires the full capacity of Trim24 to directly bind to Rara.

To further investigate the mechanism of this inhibition, we next studied the recruitment of Trim24 and Rara to the *Stat1* promoter region using ChIP technology. As a control, we examined in parallel the binding of Trim24 and Rara to a well characterized RA target, the *Cyp26a1* promoter (17). Although Rara was shown to occupy RARE of the endogenous *Stat1* promoter both in the presence and absence of RA, we observed a ligand-dependent recruitment of Trim24 to *Stat1* RARE (Fig. 4*B*). This recruitment was not observed for Trim24L730A/L731A whose capacity to interact with Rara was abolished (Fig. 4*B*). Similar results were obtained on the *Cyp26a1* RARE, validating the reliability of the technology used and the promoter occupancies (Fig. 4*B*). Taken together, these results show that Trim24 is a direct repressor of RA-mediated transactivation of the *Stat1* gene and therefore a negative regulator of the IFN/STAT signaling pathway through Rara inhibition.

DISCUSSION

In the present study, we aimed to further characterize the molecular functions of the Trim24 tumor suppressor protein as well as to identify Trim24 targets genes. Among them, Rara-dependent targets should likely include those controlling hepatocyte proliferation and hepatocarcinogenesis because deletion of a single *Rara* allele in a Trim24-null background completely reverses spontaneous liver tumor development (16, 17). Transcriptomics analyses at different stages of the disease revealed Rara-dependent overexpression of 66 and 129 components of the IFN/STAT pathway upon loss of *Trim24* at week 5 and in HCC, respectively. By performing ChIP experiments in a murine hepatic cell line (AML12), we demonstrated that Rara is bound to a RARE element of the *Stat1* promoter. Hence, upon RA treatment, Rara can directly activate *Stat1* transcription and consequently IFN/STAT signaling pathway in hepatic cells. However, in the presence of RA, Trim24 was also recruited to the *Stat1* RARE and attenuated this RA-mediated activation. This recruitment and consequent inhibition of transcription required the ability of Trim24 to interact with Rara. Therefore, we identified Trim24 as a novel negative regulator of the IFN/STAT signaling pathway acting through Rara inhibition (see the model in Fig. 5). Our model is based on the presence of an active IFN/STAT pathway in the liver cells, which was confirmed by the detection of Ser-727 phosphorylated Stat1 as well as *Ifna* and *Ifng* expression in livers of every studied genotype (Fig. 2*B*). Although it has been established that RA can synergize with IFNs to induce the expression of Stat1 targets, it is to our knowledge the first time that an activation of RA signaling has been described to be sufficient to activate the IFN/STAT signaling pathway.

Molecules inducing IFN/STAT antiviral activity are administered to treat viral hepatitis and are thought to participate to antitumoral defense in HCC. However, four observations emphasize the need to carefully re-evaluate the use of these drugs in regard to their possible involvement in liver tumor promotion. (i) Overactivation of the IFN/STAT pathway was very pronounced in *Trim24* KO HCC. In total, 129 genes of the pathway were found to be deregulated in the sense of the acti-

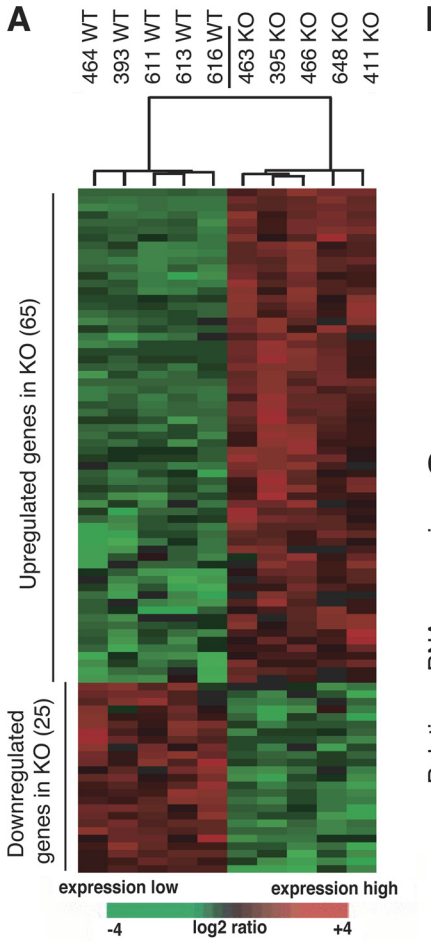

B

Interferon signaling genes deregulated in week 14 *Trim24*$^{-/-}$(KO) livers

Gene symbol	Probe set	Gene name	FC
2810474019Rik	1429558_at	RIKEN cDNA 2810474019 gene	5.78
Ifi204	1419603_at	Interferon activated gene 204	5.25
S100a11	1460351_at	S100 calcium binding protein A11 (calgizzarin)	3.66
Usp18	1418191_at	Ubiquitin specific peptidase 18	2.40
Large	1417435_at	Like-glycosyltransferase	2.38
C3ar1	1442082_at	Complement component 3a receptor 1	1.99
Foxa2	1422833_at	Forkhead box A2	1.94
Oas1a	1424775_at	2-5 oligoadenylate synthetase 1A	1.84
Glul	1426235_a_at	Glutamate-ammonia ligase	0.52
Oat	1416452_at	Ornithine aminotransferase	0.50

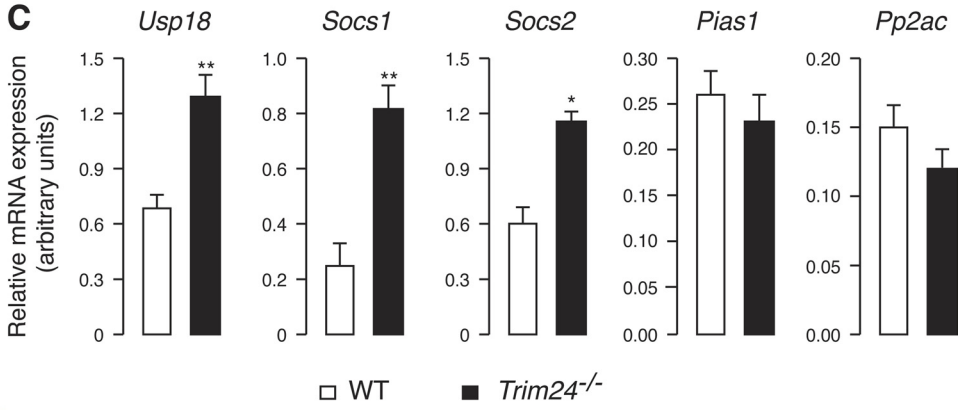

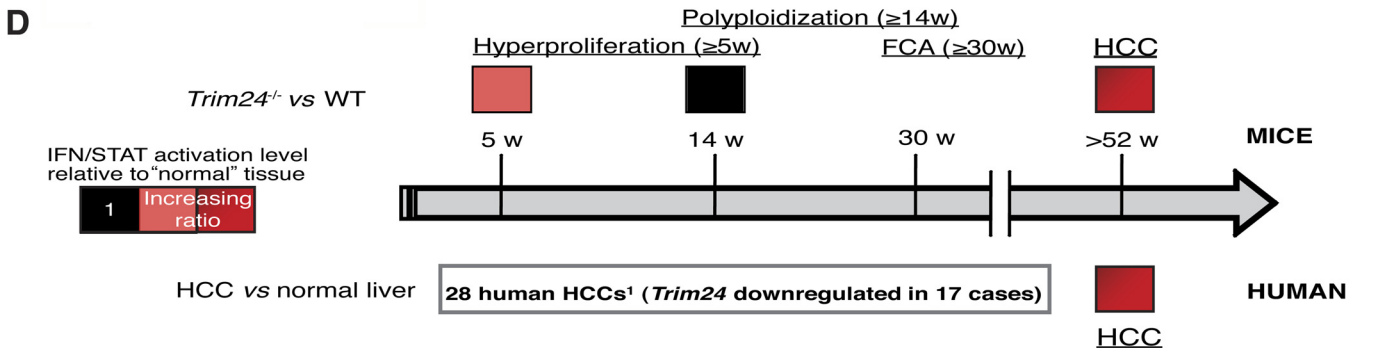

FIGURE 3. **Evolution of transcriptomes of Trim24-deficient mice during hepatocarcinogenesis and comparison with human HCCs.** *A*, average linkage hierarchical clustering of the 90 genes that were significantly deregulated in week 14 *Trim24*$^{-/-}$ (KO) liver samples. Each *column* represents a liver sample, and each *row* represents a gene. *Red* and *green* represent up- and down-regulation, respectively. *B*, genes involved in the IFN response deregulated in week 14 *Trim24* KO livers. A list of genes up- or down-regulated by a factor >1.7 ($p \leq 0.01$) found in the IFN-regulated gene database is shown. -Fold change values (*FC*) correspond to averages of all the KO/WT sample comparisons ($n = 5$). *C*, expression analysis of *Usp18*, *Socs1*, *Socs2*, *PIAS1*, and *Pp2ac* by qPCR in livers of week 14 WT and *Trim24*$^{-/-}$ mice ($n = 4$). Expression was analyzed in triplicate and normalized to *Hprt* level (*Error bars* represent standard error; *, $p < 0.005$; **, $p < 0.001$). *D*, IFN/STAT overactivation during hepatocarcinogenesis in mice and humans. A summarizing scheme representing the activation levels of the IFN/STAT pathway relative to normal hepatic tissue at different stages of liver disease in Trim24-deficient mice (*upper part*) and in 28 cases of human HCCs (*lower part*) described by Breuhahn *et al.* (38) is shown. The IFN/STAT pathway was up-regulated in hyperproliferating Trim24-deficient hepatocytes at week (*w*) 5, but a normal (WT) level was reestablished at week 14 when increased hepatocyte ploidy was observed in Trim24 KO livers. The IFN/STAT pathway was dramatically activated in all HCCs from Trim24-deficient mice as well as in 28 cases of human HCCs for which Trim24 underexpression is considered as a part of their transcriptional signature (38). *Footnote 1*, according to Breuhahn *et al.* (38).

vation of the pathway (*i.e.* up-regulation of activators and target genes and down-regulation of repressors). (ii) This overactivation took place very early in tumorigenesis (5 weeks) and is highly correlated to the tumor-promoting activation of RA signaling as revealed by the time course of gene deregulations in *Trim24*$^{-/-}$ livers. (iii) Tumor suppressors and growth inhibitors (*p21*, *Bmyc*, and *Hnf6/Onecut*) were induced together with IFN/STAT pathway repressors (*Usp18*, *Socs1*, and *Socs2*) following initial activation of the pathway. This resulted in a marked attenuation of the IFN/STAT pathway (week 14) and strongly suggests the existence of protective mechanisms to fight against deleterious effects of these overactivations on liver

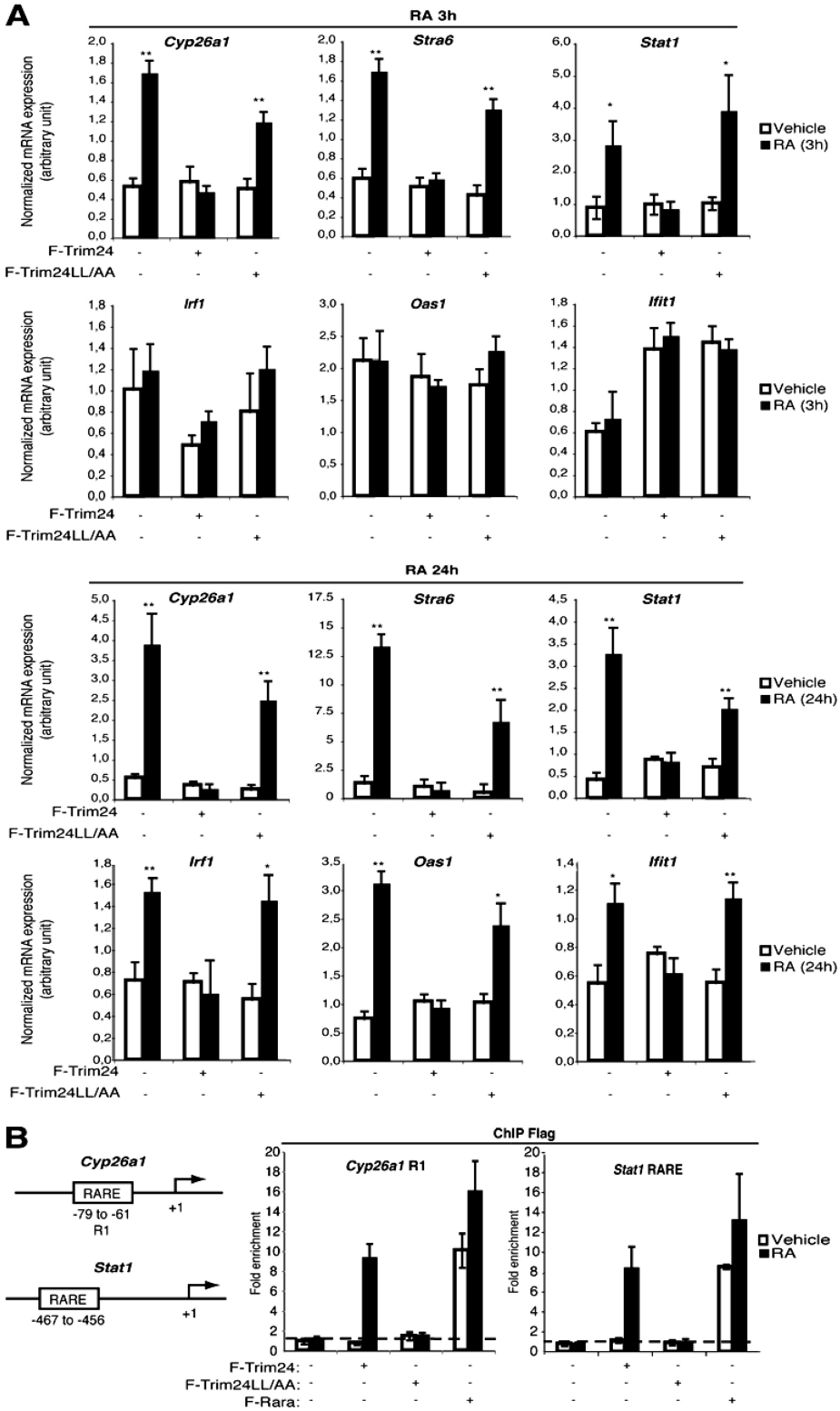

FIGURE 4. **Trim24 functions as a repressor of IFN/STAT pathway induction by RA in liver-derived AML12 cells.** *A*, forced expression of Trim24 in AML12 cells inhibits RA-dependent transactivation of IFN pathway genes. AML12 cells (2×10^6) were transfected using the Amaxa Nucleofactor (Amaxa Biosystems, Lonza) with pSG5-based expression vectors for Rara (0.125 μg) and Rxra (0.125 μg) together with a control empty vector, F-Trim24, or F-Trim24L730A/L731A defective in Rara interaction (*F-Trim24LL/AA*) (4.75 μg). Cells were treated with RA or vehicle for 3 (*top*) or 24 h (*bottom*). Expression was analyzed by qPCR in triplicate and normalized to *Hprt* level (*Error bars* represent standard error; *, $p < 0.05$; **, $p < 0.005$). *B*, ligand-dependent recruitment of Trim24 to the RARE region of *Stat1* promoter. *Left*, schematic representation of *Cyp26a1* and *Stat1* promoters. *Right*, anti-FLAG ChIP from AML12 cells transfected with either a control empty vector (−), F-Trim24 (+), F-Trim24L730A/L731A, or F-Rara together with Rara and Rxra. Immunoprecipitated and input materials were analyzed by qPCR using primers specific for the RARE-containing regions of *Cyp26a1* (positive control) and *Stat1*. Results shown as relative enrichments as compared with *Hprt* (negative control; *horizontal line*) are the mean of three independent experiments, each performed in triplicate (*Error bars* represent standard error; *, $p < 0.05$).

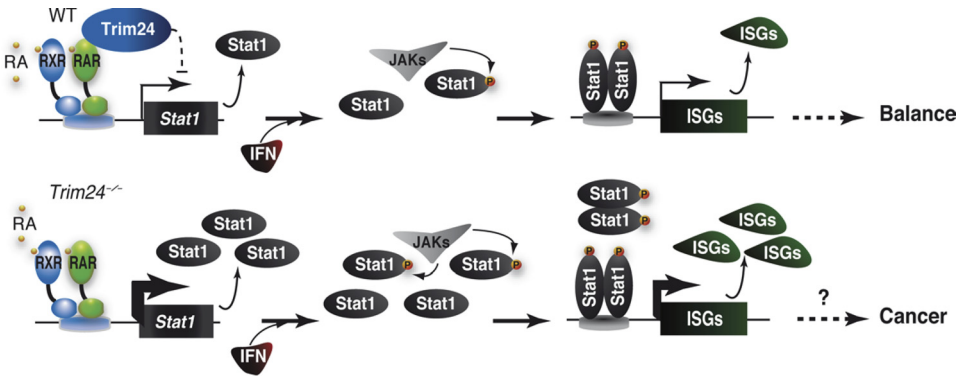

FIGURE 5. **Model of Trim24 limiting IFN/STAT pathway through inhibition of Rara activity.** *RXR*, retinoid X receptor.

homeostasis. (iv) The early up-regulation of the IFN/STAT pathway was not observed in *Trim24*$^{-/-}$*Rara*$^{+/-}$ livers, which are not prone to tumor development. All these results suggest that the IFN/STAT pathway could favor hepatocarcinogenesis. In agreement with this idea, interferon treatment of some human patients has been shown to result in the rapid growth of HCC (40). Altogether, these data suggest that the IFN/STAT pathway is an evolutionarily conserved promoter of hepatocarcinogenesis. In support to this, the IFN/STAT pathway has been proposed to be oncogenic (41–45). In particular, in gastric and colorectal cancer models, restoring a normal activation level of Stat1 results in reduction or suppression of carcinogenesis (44, 45).

Several other correlative studies demonstrate the involvement of the IFN/STAT pathway in hepatocarcinogenesis. The human HCC marker Fat10 was demonstrated to be induced by TNFα/IFNγ synergy (46). More strikingly, Yoshikawa *et al.* (47) first reported that *SOCS1* is often silenced by methylation in human HCC and shows growth-suppressive activity, suggesting the requirement of a constitutively activated STAT pathway in the development of human HCC. These discoveries are consistent with the down-regulation of *Socs1* that we observed in *Trim24* KO HCC as well as with its overexpression at week 14 as a probable feedback. Furthermore, a genetic study revealed that IFNγ is critically involved in the initiation stage of chemically induced hepatocarcinogenesis (48). Most importantly, gene expression profiling of 43 human HCCs revealed that 65% of these tumors exhibit overexpression of ISGs (38). Interestingly, we noticed that Trim24 down-regulation is part of a highly discriminative transcriptional signature of this tumor subgroup. The correlation between IFN/STAT activation and Trim24 underexpression in these HCCs strongly supports our proposal and once more suggests that basic mechanisms of hepatocarcinogenesis are evolutionarily conserved.

However, it still remains elusive which steps of carcinogenesis are controlled by IFN/STAT pathway. Mice lacking Socs1 display an increased Stat1 activation level and spontaneously develop colorectal carcinomas, a phenotype suppressed by concomitant *Ifng* inactivation (44). The observation that these animals display an elevated intestinal epithelium proliferation level even in non-tumoral tissues (44) suggests that overactivation of IFN/STAT pathway could be mitogenic. On the other hand, recent works on aggressive tumor clones revealed that IFN/STAT activation promotes metastatic potential and resistance to chemotherapy and radiation (49, 50). Indeed, stable knockdown of Stat1 reversed the aggressive phenotype and decreased both colonization and resistance to therapy (50). Therefore, the IFN/STAT pathway seems to be involved in different stages of carcinogenesis. This is in good agreement with our discoveries showing IFN/STAT activation in both pretumoral hyperproliferating livers (week 5) and HCCs and underlines the crucial importance of a balanced IFN/STAT signaling.

Molecular mechanisms leading to tumorigenesis following abnormal IFN/STAT activation remain to be clarified, but several mediators could be proposed based on very recent reports. The Isg15/Herc5/Usp18 pathway is activated by IFN/STAT signaling and modulates various cellular processes, including immune response by deubiquitination and prevention of degradation (51). In tumors, activation of this pathway is a marker of chemo- and IFN resistance (51). In the liver it is exploited by hepatitis C virus to evade the immune response and was demonstrated to inhibit the apoptotic effect of Type I IFN (51, 52). Interestingly, all three IFN/STAT-inducible components of this pathway were overexpressed in a Rara-dependent manner in week 5 *Trim24*$^{-/-}$ livers (*Isg15*, 7.54-fold; *Herc5*, 5.98-fold; and *Usp18*, 4.88-fold) and tumors (10.17-, 4.79-, and 3.69-fold, respectively). Therefore, it is tempting to speculate that activation of this pathway might be established in *Trim24* KO HCC to circumvent IFN/STAT antitumoral activity. Moreover, Usp18 has been recently demonstrated to enhance epidermal growth factor receptor (EGFR) mRNA translation, thus promoting tumorigenic activity, cancer cell survival, and cell proliferation (53). This discovery hence makes Usp18 an interesting candidate for mediating IFN/STAT-induced hepatocarcinogenesis in Trim24 KO mice.

Additional genetic experiments are required to fully establish IFN/STAT pathway as oncogenic in the liver. Mice lacking Stat1 show hypersensitivity to opportunistic infections (especially mycobacterial infection) but are otherwise normal, do not present any developmental defect, and are indistinguishable from their WT littermates in a pathogen-free environment (54, 55). The generation of *Trim24*/*Stat1* double knock-out mice (work in progress) and the investigation of their liver phenotype should represent a decisive step to characterize the oncogenic potential of the IFN/STAT signaling pathway in the liver. Interestingly, an anti-IFNγ antibody that is being tested in patients for Crohn disease has been proposed as a candidate molecule for the inhibition of the IFN/STAT pathway in colorectal can-

cers (56). It would be very interesting to assess the effect of this antibody on HCC development in Trim24-deficient mice.

In the present study, we identified Trim24, known as Tif1α, as a novel negative regulator of the IFN/STAT signaling pathway acting via Rara inhibition and uncovered a novel therapeutical target for the prevention and/or treatment of liver carcinogenesis. In this respect, the *Trim24* KO mouse line should represent a valuable tool for developing new therapeutic strategies and evaluating drug safety.

Acknowledgments—We are grateful to Carme Caelles Franch for support and discussions, Laeticia Walsh for technical help at the Animal House, and the Institut de Génétique et de Biologie Moléculaire et Cellulaire common facilities.

REFERENCES

1. Huynh, H. (2010) *Biochem. Pharmacol.* **80,** 550–560
2. Trevisani, F., Cantarini, M. C., Wands, J. R., and Bernardi, M. (2008) *Carcinogenesis* **29,** 1299–1305
3. Kensler, T. W., Qian, G. S., Chen, J. G., and Groopman, J. D. (2003) *Nat. Rev. Cancer* **3,** 321–329
4. Coulouarn, C., Factor, V. M., and Thorgeirsson, S. S. (2008) *Hepatology* **47,** 2059–2067
5. Thorgeirsson, S. S., Lee, J. S., and Grisham, J. W. (2006) *Hepatology* **43,** S145–150
6. Miki, T., Fleming, T. P., Crescenzi, M., Molloy, C. J., Blam, S. B., Reynolds, S. H., and Aaronson, S. A. (1991) *Proc. Natl. Acad. Sci. U.S.A.* **88,** 5167–5171
7. Le Douarin, B., Zechel, C., Garnier, J. M., Lutz, Y., Tora, L., Pierrat, P., Heery, D., Gronemeyer, H., Chambon, P., and Losson, R. (1995) *EMBO J.* **14,** 2020–2033
8. Le Douarin, B., Nielsen, A. L., Garnier, J. M., Ichinose, H., Jeanmougin, F., Losson, R., and Chambon, P. (1996) *EMBO J.* **15,** 6701–6715
9. Nielsen, A. L., Ortiz, J. A., You, J., Oulad-Abdelghani, M., Khechumian, R., Gansmuller, A., Chambon, P., and Losson, R. (1999) *EMBO J.* **18,** 6385–6395
10. Beckstead, R., Ortiz, J. A., Sanchez, C., Prokopenko, S. N., Chambon, P., Losson, R., and Bellen, H. J. (2001) *Mol. Cell* **7,** 753–765
11. Zhong, S., Delva, L., Rachez, C., Cenciarelli, C., Gandini, D., Zhang, H., Kalantry, S., Freedman, L. P., and Pandolfi, P. P. (1999) *Nat. Genet.* **23,** 287–295
12. Teyssier, C., Ou, C. Y., Khetchoumian, K., Losson, R., and Stallcup, M. R. (2006) *Mol. Endocrinol.* **20,** 1276–1286
13. Tsai, W. W., Wang, Z., Yiu, T. T., Akdemir, K. C., Xia, W., Winter, S., Tsai, C. Y., Shi, X., Schwarzer, D., Plunkett, W., Aronow, B., Gozani, O., Fischle, W., Hung, M. C., Patel, D. J., and Barton, M. C. (2010) *Nature* **468,** 927–932
14. Chambon, P. (2005) *Mol. Endocrinol.* **19,** 1418–1428
15. Chelbi-Alix, M. K., and Pelicano, L. (1999) *Leukemia* **13,** 1167–1174
16. Khetchoumian, K., Teletin, M., Tisserand, J., Mark, M., Herquel, B., Ignat, M., Zucman-Rossi, J., Cammas, F., Lerouge, T., Thibault, C., Metzger, D., Chambon, P., and Losson, R. (2007) *Nat. Genet.* **39,** 1500–1506
17. Khetchoumian, K., Teletin, M., Tisserand, J., Herquel, B., Ouararhni, K., and Losson, R. (2008) *Cell Cycle* **7,** 3647–3652
18. Herquel, B., Ouararhni, K., Khetchoumian, K., Ignat, M., Teletin, M., Mark, M., Béchade, G., Van Dorsselaer, A., Sanglier-Cianférani, S., Hamiche, A., Cammas, F., Davidson, I., and Losson, R. (2011) *Proc. Natl. Acad. Sci. U.S.A.* **108,** 8212–8217
19. Desmet, V. J. (2009) *Hepatology* **49,** 355–357
20. Khetchoumian, K., Teletin, M., Mark, M., Lerouge, T., Cerviño, M., Oulad-Abdelghani, M., Chambon, P., and Losson, R. (2004) *J. Biol. Chem.* **279,** 48329–48341
21. Wu, J. C., Merlino, G., and Fausto, N. (1994) *Proc. Natl. Acad. Sci. U.S.A.* **91,** 674–678
22. Kolla, V., Weihua, X., and Kalvakolanu, D. V. (1997) *J. Biol. Chem.* **272,** 9742–9748
23. Loudig, O., Babichuk, C., White, J., Abu-Abed, S., Mueller, C., and Petkovich, M. (2000) *Mol. Endocrinol.* **14,** 1483–1497
24. Platanias, L. C. (2005) *Nat. Rev. Immunol.* **5,** 375–386
25. Samarajiwa, S. A., Forster, S., Auchettl, K., and Hertzog, P. J. (2009) *Nucleic Acids Res.* **37,** D852–D857
26. Taniguchi, T., Ogasawara, K., Takaoka, A., and Tanaka, N. (2001) *Annu. Rev. Immunol.* **19,** 623–655
27. Sherr, C. J., and Roberts, J. M. (1999) *Genes Dev.* **13,** 1501–1512
28. Resar, L. M., Dolde, C., Barrett, J. F., and Dang, C. V. (1993) *Mol. Cell Biol.* **13,** 1130–1136
29. Lehner, F., Kulik, U., Klempnauer, J., and Borlak, J. (2007) *FASEB J.* **21,** 1445–1462
30. Lehner, F., Kulik, U., Klempnauer, J., and Borlak, J. (2010) *PLoS One* **5,** e13344
31. Wu, H., Wade, M., Krall, L., Grisham, J., Xiong, Y., and Van Dyke, T. (1996) *Genes Dev.* **10,** 245–260
32. Gupta, S. (2000) *Semin. Cancer Biol.* **10,** 161–171
33. Balmer, J. E., and Blomhoff, R. (2002) *J. Lipid Res.* **43,** 1773–1808
34. Sarasin-Filipowicz, M., Wang, X., Yan, M., Duong, F. H., Poli, V., Hilton, D. J., Zhang, D. E., and Heim, M. H. (2009) *Mol. Cell. Biol.* **29,** 4841–4851
35. Krebs, D. L., and Hilton, D. J. (2001) *Stem Cells* **19,** 378–387
36. Liu, B., Liao, J., Rao, X., Kushner, S. A., Chung, C. D., Chang, D. D., and Shuai, K. (1998) *Proc. Natl. Acad. Sci. U.S.A.* **95,** 10626–10631
37. Duong, F. H., Christen, V., Berke, J. M., Penna, S. H., Moradpour, D., and Heim, M. H., (2005) *J. Virol.* **79,** 15342–15350
38. Breuhahn, K., Vreden, S., Haddad, R., Beckebaum, S., Stippel, D., Flemming, P., Nussbaum, T., Caselmann, W. H., Haab, B. B., and Schirmacher, P. (2004) *Cancer Res.* **64,** 6058–6064
39. Kolla, V., Lindner, D. J., Xiao, W., Borden, E. C., and Kalvakolanu, D. V. (1996) *J. Biol. Chem.* **271,** 10508–10514
40. Onitsuka, A., Yamada, N., Yasuda, H., Miyata, T., and Kachi, T. (1996) *Surg. Today* **26,** 126–130
41. Bromberg, J. (2002) *J. Clin. Investig.* **109,** 1139–1142
42. Buettner, R., Mora, L. B., and Jove, R. (2002) *Clin. Cancer Res.* **8,** 945–954
43. Yoshimura, A. (2006) *Cancer Sci.* **97,** 439–447
44. Hanada, T., Kobayashi, T., Chinen, T., Saeki, K., Takaki, H., Koga, K., Minoda, Y., Sanada, T., Yoshioka, T., Mimata, H., Kato, S., and Yoshimura, A. (2006) *J. Exp. Med.* **203,** 1391–1397
45. Ernst, M., Najdovska, M., Grail, D., Lundgren-May, T., Buchert, M., Tye, H., Matthews, V. B., Armes, J., Bhathal, P. S., Hughes, N. R., Marcusson, E. G., Karras, J. G., Na, S., Sedgwick, J. D., Hertzog, P. J., and Jenkins, B. J. (2008) *J. Clin. Investig.* **118,** 1727–1738
46. Lukasiak, S., Schiller, C., Oehlschlaeger, P., Schmidtke, G., Krause, P., Legler, D. F., Autschbach, F., Schirmacher, P., Breuhahn, K., and Groettrup, M. (2008) *Oncogene* **27,** 6068–6074
47. Yoshikawa, H., Matsubara, K., Qian, G. S., Jackson, P., Groopman, J. D., Manning, J. E., Harris, C. C., and Herman, J. G. (2001) *Nat. Genet.* **28,** 29–35
48. Matsuda, M., Nakamoto, Y., Suzuki, S., Kurata, T., and Kaneko, S. (2005) *Lab. Invest.* **85,** 655–663
49. Roberts, D., Schick, J., Conway, S., Biade, S., Laub, P. B., Stevenson, J. P., Hamilton, T. C., O'Dwyer, P. J., and Johnson, S. W. (2005) *Br. J. Cancer* **92,** 1149–1158
50. Khodarev, N. N., Roach, P., Pitroda, S. P., Golden, D. W., Bhayani, M., Shao, M. Y., Darga, T. E., Beveridge, M. G., Sood, R. F., Sutton, H. G., Beckett, M. A., Mauceri, H. J., Posner, M. C., and Weichselbaum, R. R. (2009) *PLoS One* **4,** e5821
51. Chen, L., Li, S., and McGilvray, I. (2011) *Int. J. Biochem. Cell Biol.,* in press
52. Potu, H., Sgorbissa, A., and Brancolini, C. (2010) *Cancer Res.* **70,** 655–665
53. Duex, J. E., Comeau, L., Sorkin, A., Purow, B., and Kefas, B. (2011) *J. Biol. Chem.* **286,** 25377–25386
54. Meraz, M. A., White, J. M., Sheehan, K. C., Bach, E. A., Rodig, S. J., Dighe, A. S., Kaplan, D. H., Riley, J. K., Greenlund, A. C., Campbell, D., Carver-Moore, K., DuBois, R. N., Clark, R., Aguet, M., and Schreiber, R. D. (1996) *Cell* **84,** 431–442
55. Sugawara, I., Yamada, H., and Mizuno, S. (2004) *Tohoku J. Exp. Med.* **202,** 41–50
56. Grivennikov, S. I., Greten, F. R., and Karin, M. (2010) *Cell* **140,** 883–899